

# Impact of Global Data Assimilation System atmospheric models on astroparticle showers

J. Grisales-Casadiegos, C. Sarmiento-Cano, and L.A. Núñez and the LAGO Collaboration

**Abstract:** We present a methodology to simulate the impact of the atmospheric models in the background particle flux on ground detectors using the Global Data Assimilation System. The methodology was within the ARTI simulation framework developed by the Latin American Giant Observatory Collaboration. The ground level secondary flux simulations were performed with a tropical climate at the city of Bucaramanga, Colombia. To validate our methodology, we built monthly profiles over Malargüe between 2006 and 2011, comparing the maximum atmospheric depth,  $X_{\max}$ , with those calculated with the Auger atmospheric option in CORSIKA. The results show significant differences between the predefined CORSIKA atmospheres and their corresponding Global Data Assimilation System atmospheric profiles.

## 1. Introduction

The interaction of cosmic rays with the nuclei of atomic elements in the atmosphere produces a cascade of particles: the extensive air shower (EAS). These cascades, measured at the Earth's surface, result from an intricate convolution of physical phenomena: including dispersion, decay and absorption of high energy particles crossing the atmosphere. For energies below  $10^{12}$  eV, the primaries are modulated by the solar wind. Thus they interact with the interplanetary and geomagnetic fields, resulting in what is known as Space Weather Physics. An excellent overview of this exciting field can be found in [1, 2, 3, 4] and references therein.

The Latin American Giant Observatory (LAGO) is an astroparticle observatory with water Cherenkov detectors (WCD) distributed from Mexico to Antarctica, covering a broad range of geomagnetic rigidity cutoffs and atmospheric depths (from sea level up to more than 5000 m.a.s.l. [5]). LAGO has developed a Space Weather program [6] to explore the influence of space climate on the cosmic ray flux at ground level. This research program has developed a precise simulation scheme, taking into account the geomagnetic corrections, providing an estimation of the response of a Water Cherenkov Detector (WCD) to the impinging particle flux at any geographic place on Earth's surface [7]. The simulation

**Jennifer Grisales-Casadiegos.** Escuela de Física, Facultad de Ciencias, Universidad Industrial de Santander, Bucaramanga, Bucaramanga, 680002, Colombia. jennifer.grisales@saber.uis.edu.co

**Christian Sarmiento-Cano.** Instituto de Tecnología Sabato, Universidad Nacional de San Martín, Centro Atómico Constituyentes, and Instituto en Tecnologías de Detección y Astropartículas, Buenos Aires, Argentina

**Luis A. Núñez.** Escuela de Física, Facultad de Ciencias, Universidad Industrial de Santander, Bucaramanga, 680002, Colombia and Departamento de Física, Facultad de Ciencias, Universidad de Los Andes, Mérida 5101, Venezuela

pipeline of computing algorithms considers three factors with different spatial and time scales: the geomagnetic effects, the development of the extensive air showers in the atmosphere, and the detector response at ground level.

In this work we use GDASTOOL –a python routine based on the Global Data Assimilation System (GDAS) [8]– as part of a methodology use in creating monthly atmospheric profiles for any location. This routine is available in the latest versions of CORSIKA (Cosmic Ray Simulations for KASCADE <sup>1</sup>) and allows us to obtain a specific atmosphere model for a particular day, time and geographic location. GDASTOOL helps us visualize the impact that detailed atmospheric and climate models have on the cosmic ray flux at the Earth’s surface.

We show the usefulness these profiles have in reproducing the atmospheric conditions in which an EAS develops. Also, by applying the described methodology to the city of Bucaramanga-Colombia, we determined the influence of the monthly atmospheric models on the flux of secondary particles arriving at the LAGO WCD detectors. With this insight, we discuss the relevance of implementing GDAS at any geographical location.

This work is organized as follows: In the next section, we briefly describe the Latin American Giant Observatory and present the structure of the ARTI computational framework. In section 3, we discuss the methodology used to build the atmospheric models and the GDAS implementation at the Pierre Auger Observatory. Then, in section 4 we present the results obtained by comparing the background flux reaching the surface using the standard tropical atmosphere versus the GDAS atmospheres. Finally we will end with some remarks displayed in section 5.

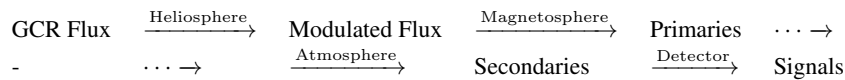
## 2. LAGO and the ARTI simulation framework

The Latin American Giant Observatory is an extended observatory on a continental scale, promoting training and research in astroparticle physics in Latin America. Its three main research areas are space weather phenomena, search for gamma rays bursts at high altitude sites and background radiation at ground level.

The LAGO WCD detection network extends over several sites at different latitudes and altitudes, covering various geomagnetic rigidity and atmospheric depths. The low-cost LAGO WCDs have proven detection reliability and efficiency for both electromagnetic and muon EAS components [5].

The LAGO Space Weather Program studies the relation between the variation in the flux of secondary particles at ground level with the heliospheric modulation of Galactic Cosmic Rays (GCR). Through the multi-spectral analysis technique [6], LAGO provides detailed information of the temporal evolution of the secondary flux at different geomagnetic locations, contributing to a better understanding better in the disturbances produced by different space weather phenomena [9].

The estimation of the expected flux of secondaries at any detector of the LAGO network is based on a detailed and realistic simulation considering all possible sources of flux variation. This complex approach involving processes occurring at different spatial and time scales, can be depicted as:



The above simulation scheme considers three essential factors with different spatial and time scales: the geomagnetic effects, the development of the extensive air showers in the atmosphere, and the detector response at ground level [10].

---

<sup>1</sup> KASCADE: KARlsruhe Shower Core and Array DEtector

To take into account all these elements, we use ARTI: a complete computational framework for estimating the signals expected at the WCD detector and involving three main simulation blocks. [11, 12]:

1. The effects of the Geomagnetic Field (GF) on the propagation of charged particles, contributing to the background radiation at ground level, is characterized by the directional rigidity cutoff,  $R_C$ . This is performed at each LAGO site, using the MAGNETOCOSMICS code [13], applying the backtracking technique [14]. The GF at any point on Earth is determined by using the International Geomagnetic Field Reference, version 11 [15] at the near-Earth GF ( $r < 5R_\oplus$ )<sup>2</sup> and through the Tsyganenko Magnetic Field model version 2001 (TSY01 hereafter) [16] to describe the outer GF ( $r > 5R_\oplus$ ).
2. The second block simulates the extensive air showers produced during the interaction of cosmic rays with the atmosphere, obtaining a comprehensive set of secondaries at ground level. This block uses the CORSIKA (currently v7.6400) code [17], compiled with the following options: QGSJET-II-04 [18], GHEISHA-2002, EGS4, curved and external atmosphere, and volumetric detector.
3. Finally, with GEANT4, we model [19] the detector response to the different types of impinging secondary particles obtaining the distribution of photo-electrons for a particular type of detector. The response of the WCD detectors is estimated by considering the detector geometry, e.g. cylindrical containers of water with an inner coating made of Tyvek® [20], and a single photo-multiplier tube (PMT, Hamamatsu R5912) located at the centre and top of the cylinder [21].

For simplicity, we have presented the above blocks as consecutive, but we sketched the precise ARTI operational pseudo-code in the Appendix. For a more detailed description, we refer the interested reader to the original paper [12].

The first two blocks have been integrated into a dedicated Virtual Organization, *lagoproject*, as part of the European Grid Infrastructure (EGI, <http://www.egi.eu>) activities. The Grid implementation of CORSIKA was deployed with two “flavours”, which run using GridWay Metascheduler (<http://www.gridway.org/doku.php>) [22]. Massive calculations can be executed with the former, via the Montera [23], the GWpilot [24], the GWcloud [25] and recently the EOSC-Synergy cloud services [26] frameworks.

### 3. Atmospheric models with GDAS for the background study of secondary

Understanding the propagation of EAS is decisive in estimating the flux of secondary particles at the detectors on the surface of the Earth. Therefore we must accurately characterize the atmosphere to simulate correctly the corresponding processes involved. One of the essential atmosphere parameters is density, which determines the probability of interaction as the EAS evolves. The atmospheric density is concentrated in the first 30 km from the ground up, decreasing as the altitude increases.

In this case, the atmospheric density is modelled by the vertical depth [27], measured in  $\text{g/cm}^2$  and defined as

$$X_h = \int_h^\infty \rho(h') dh', \quad (1)$$

where  $\rho(h)$  is the density as a function of height,  $h$ , above the Earth.

---

<sup>2</sup> $r$  distance from Earth center and  $R_\oplus$  is the Earth radius (6371 km).

From the ground up, five density layers model describe the atmosphere (i.e. Lindsley's standard atmospheric model [28]), and an exponential can approximate the first four:

$$X_h = a_i + b_i e^{\frac{-h}{c_i}} \quad i = 1, \dots, 4. \quad (2)$$

At the same time the vertical atmospheric depth decreases linearly with height as

$$X_h = \alpha_s - \beta_s \frac{h}{\eta_s}; \quad (3)$$

where  $a_i$ ,  $b_i$ ,  $c_i$ ,  $\alpha_s$ ,  $\beta_s$  and  $\eta_s$  are the corresponding parameters of each atmospheric layer, which should be continuous across the boundaries of the different atmospheric segments [17, 29].

### 3.1. EAS, CORSIKA and GDAS

CORSIKA applies Monte Carlo algorithms for EAS simulations and recreates its propagation when initiated by protons, photons, nuclei, or any other incoming particles [17]. CORSIKA models the atmosphere through different types of configurations with a certain level of detail:

- ATMOD establishes predefined atmospheric models for specific locations, given the values of the parameters for each atmospheric layer.
- ATMEXT is a configuration for external atmospheres dependent on the geographical location, with the most common implemented models: tropical, mid-latitude summer, mid-latitude winter, sub-arctic summer, sub-arctic winter and U.S standard atmosphere at the South pole.
- Finally, the ATMFILE configuration lets us input a GDAS profile file previously created using the GDASTOOL code available in the CORSIKA software.

The configuration implemented for this work is ATMFILE Datacard using GDASTOOL [17], which allow us to create an atmospheric model from GDAS. The GDAS atmospheric model incorporates the behaviour of the atmosphere based on meteorological observations (National Archive and Distribution System for Operational Models, NOAA).

GDAS builds realistic climate predictions, describing the state of the atmosphere for certain variables in time and altitude. At a given time,  $t_0$ , the observations give a value for a state variable, and at the same time, a forecast is available. The analysis stage combines observation and prediction to improve the model at  $t_0$ . After curve fitting, a forecast is made for a later time  $t_1$  [29].

However, it is not enough to have an atmospheric profile for a given day and time to estimate the averaged secondary flux over any geographic location. A more robust model needs to be built, containing sufficient climate information over a given time interval. In this regard, previous studies have demonstrated the utility of building monthly GDAS atmospheric profiles on the CORSIKA's simulations [30].

Therefore, in this work, we propose a methodology that uses CORSIKA's GDASTOOL to extract an atmospheric profile for a specific day and time and build monthly average atmospheric profiles. GDASTOOL extracts values for the pressure, altitude, temperature and humidity, from GDAS-NOAA databases then fit them into the five-layer model implemented in CORSIKA [17, 29].

### 3.2. Monthly atmospheric profiles

To build monthly atmospheric profiles, we implemented a computational algorithm using GDAS-TOOL that extracts data twice daily: at 0:00h and 12:00h, for all days of a year at any geographic

position. In our case, as displayed in figure 1, it is for the city of Bucaramanga-Colombia ( $7.13^\circ$  N,  $73.00^\circ$  W).

We extracted 730 profiles per year, i.e. two profiles per day. Figure 2 (left plate) shows all the instantaneous profiles for January 2018 (solid line) and their average (dash line). As can be seen, some differences appear between them, although they highly agree in the initial 30 km.

Thus, we built 12 monthly profiles for the year 2018 in the city Bucaramanga-Colombia and compared them with the predetermined profiles for this location (tropical summer/mid-latitude summer). Then, the new monthly atmospheric profile are the point-to-point average across the atmosphere over 60 daily profiles. We observed significant differences, as shown on the right plate of figure 2. Here, we plot the first 30 km, which accounts for most of the atmospheric matter density.

### 3.3. Validating the method

After obtaining the average atmospheric profiles, we must check if they reproduce the behaviour of the atmosphere in the middle of an EAS. Thus, we should apply this methodology to a location where the accuracy of GDAS was already known.

The selected location was the village of Malargüe-Argentina, where the Pierre Auger Observatory is situated. This Observatory compared the GDAS data with local measurements (atmospheric soundings with weather balloons and ground-based weather stations), validating the accuracy of GDAS for the horizontal and vertical as well as temporal resolution[29].

To validate our models, we built atmospheric profiles for Malargüe between 2006 and 2011, extracting 10-month profiles every year on April the 6th, 12th, 18th, 24th and 30th, two per day, at 0:00h and 12:00h every day.

We then compare the evolution of the EAS using our GDAS model and the Auger atmospheric model, available as a predefined option in CORSIKA. We performed 100 EAS simulations for Iron primaries of  $1 \times 10^8$  GeV. We made this choice due to two facts: the energy value should be in the maximum efficiency range, and the computation time of the simulation should not exceed one week of wall-clock time in our computational system.

From the simulations and the analysis of the longitudinal development of the EAS, we identify the  $X_{\max}$  corresponding to the maximum value of atmospheric depth, i.e. where the number of secondary particles is maximum. The  $X_{\max}$  is a crucial parameter because it is proportional to the logarithm of the mass of the primary that started the EAS [31]. We have validated our methodology, by checking if the simulations yield a value of  $X_{\max}$  close to those obtained by Pierre Auger Observatory profile. As it can be seen in figure 3, the differences in this parameter did not exceed 2%.

## 4. Particle flux and atmospheric models

First, we established the time needed to integrate the primary flux. For example, in the case of a 120-second flux, we calculated the total number of incident primaries and simulated each individual shower generated in the atmosphere. Table 1 (Appendix), shows the various primary particle contributing to the flux. The distribution corresponds to the abundances of the atomic nuclei reported in the literature [27].

Then we defined the initial conditions in order to run a series of simulations, which in our case, for the city of Bucaramanga, were established as:

- Horizontal and vertical components of the Earth's magnetic field corresponding to 27.026 nT and 17.176 nT, respectively.
- Observation level, 950 m a.s.l. for Bucaramanga.
- Primary: Nuclei from Hydrogen to Iron
- Energy range of primaries: from 5 GeV to  $10^6$  GeV.

- Zenit angle of incidence of the primaries: from  $0^\circ$  to  $90^\circ$ .
- Flux time 1 day = 86400 s.
- Type of detection: Volumetric.
- Atmospheric profile: Default tropical (mid-latitude summer) profile within ATMEXT routines, which is used so far for flux simulations over Bucaramanga, and the 12 monthly atmospheric profiles created from GDASTOOL.
- Energy cuts:  $E_s \geq 5$  MeV for  $\mu^\pm$ s and hadrons, and  $E_s \geq 5 \times 10^{-2}$  MeV for electrons and photons. Where  $E_s$  is the energy of secondary. These are the lower limits of the energies in this CORSIKA version.

Figure 4 displays the spectrum of secondaries and the total secondary flux, using the constructed April atmospheric profile. The neutron portion of the second hump is only significant between 0.2 GeV/c and 1 GeV/c, decreasing dramatically as the energy increases. In opposition, the muonic component increases in the same energy range, having its maximum value near 10 GeV/c.

The plot shows two humps for each curve representing the secondary particle flux. The first hump represents the electromagnetic component (electrons, positrons and photons), while the second, made up of two smaller humps, represents the flux of neutrons and muons, respectively.

We ran a total of 12 flux simulations using a GDAS monthly atmospheric profile at a time and, finally, one simulation using the CORSIKA tropical summer (mid-latitude summer) predefined profile available in ATMEXT configuration.

Figure 5 shows the total secondary flux as a function of energy at the altitude of Bucaramanga, using different atmospheric models. The black line corresponds to the simulation using the default tropical predefined profile, and the coloured lines correspond to the 12 monthly GDAS atmospheric models. As can be appreciated, there is a higher flux with the predefined atmosphere compared to the 12 monthly profiles.

## 5. Final remarks

We have devised a methodology that enables us to obtain a month-by-month averaged atmospheric profile for any geographic location. This methodology, implemented using the GDASTOOL code, extracts meteorological data for Bucaramanga at noon and midnight: (0:00h and 12:00 (UTC-5)), during a whole year. In this way, we created 12 atmospheric profiles for 2018 and compared them with predefined atmospheric profiles available in CORSIKA.

We validated this methodology, by generating atmospheric profiles for the Pierre Auger Observatory and contrasting them with the Observatory's GDAS-based models. The behaviour of the EAS obtained with the reconstructed atmosphere shows a difference of  $\approx 2\%$  in the value of the maximum atmospheric depth,  $X_{\max}$ .

It is essential to clarify that monthly atmospheric profiles over a year are not sufficient to represent the average climatic variability in the tropics. We need atmospheres that cover a more significant number of years. Thus, the observed differences suggest the importance of studying these effects in greater detail, for example, long-term climatic events such as the El Niño and La Niña phenomena.

This work completes the sequence of simulations that enables to study, in a realistic approach, the flux of secondaries that a WCD can detect at any geographical position and time of the year.

## Acknowledgements

The authors are grateful to Dr. Hernán Asorey for his constructive comments on previous versions of the manuscript. We also thank the Pierre Auger Observatory Collaboration members for their continuous engagement and support. LAN gratefully acknowledges the permanent support of Vicerrectoría

de Investigación y Extensión de la Universidad Industrial de Santander. This work has been partially carried out on the ACME cluster, which is owned by CIEMAT and funded by the Spanish Ministry of Science and Innovation project CODEC-OSE (RTI2018-096006-B-I00) with FEDER funds as well as supported by the CYTED co-founded RICAP Network (517RT0529). We also acknowledge the computational support from the Universidad Industrial de Santander (SC3UIS) High Performance and Scientific Computing Centre.

## References

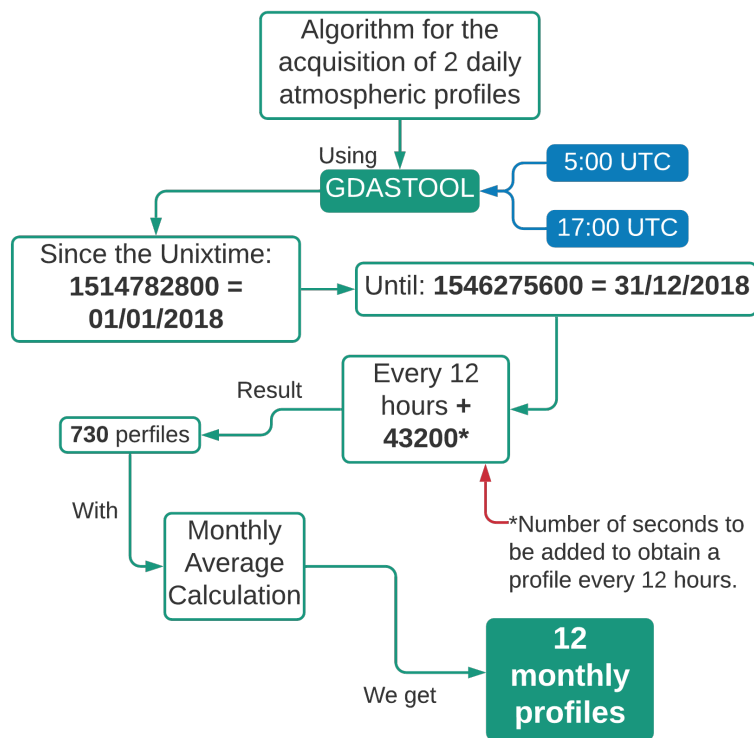
1. I.G. Usoskin, K. Mursula, S.K. Solanki, M. Schüssler, and G.A. Kovaltsov. A physical reconstruction of cosmic ray intensity since 1610. *Journal of Geophysical Research: Space Physics*, 107(A11):SSH-13, 2002.
2. V. Bothmer and I.A. Daglis. *Space weather: physics and effects*. Springer Science & Business Media, 2007.
3. L. Barnard, M. Lockwood, M.A. Hapgood, M.J. Owens, C.J. Davis, and F. Steinhilber. Predicting space climate change. *Geophysical Research Letters*, 38(16), 2011.
4. M.S. Potgieter. Solar modulation of cosmic rays. *Living Reviews in Solar Physics*, 10(1):1–66, 2013.
5. I. Sidelnik and H. Asorey. LAGO: The latin american giant observatory. *Nuclear Instruments and Methods in Physics Research Section A: Accelerators, Spectrometers, Detectors and Associated Equipment*, 876:173–175, 2017.
6. H. Asorey, S. Dasso, L.A. Núñez, Y. Pérez, C. Sarmiento-Cano, M. Suárez-Durán, and the LAGO Collaboration. The LAGO space weather program: Directional geomagnetic effects, background fluence calculations and multi-spectral data analysis. In *The 34th International Cosmic Ray Conference*, volume PoS(ICRC2015), page 142, 2015.
7. H. Asorey, L. A. Núñez, and M. Suárez-Durán. Preliminary results from the latin american giant observatory space weather simulation chain. *Space Weather*, 16(5):461–475, 2018.
8. M. Will. Global atmospheric models for cosmic ray detectors. *arXiv preprint arXiv:1402.4782*, 2014.
9. M. Suárez-Durán. *Variaciones del flujo de radiación cósmica en distintos escenarios geofísicos*. Phd thesis, School of Physics, Universidad Industrial de Santander, Bucaramanga, Colombia, December 2019.
10. H. Asorey, L.A. Núñez, M. Suárez-Durán, L.A. Torres-Niño, M. Rodríguez-Pascual, A.J. Rubio-Montero, and R. Mayo-García. The latin american giant observatory: a successful collaboration in latin america based on cosmic rays and computer science domains. In *Cluster, Cloud and Grid Computing (CCGrid), 2016 16th IEEE/ACM International Symposium on*, pages 707–711. IEEE, 2016.
11. R. Calderón-Ardila, A. Jaimes-Motta, J. Peña-Rodríguez, C. Sarmiento-Cano, M. Suárez-Durán, and A. Vásquez-Ramírez. Modeling the LAGO’s detector response to secondary particles at ground level from the Antarctic to Mexico. In *36th International Cosmic Ray Conference (ICRC2019)*, volume 36 of *International Cosmic Ray Conference*, page 412, July 2019.
12. C. Sarmiento-Cano, M. Suárez-Durán, R. Calderón-Ardila, A. Vásquez-Ramírez, A. Jaimes-Motta, S. Dasso, I. Sidelnik, L. A. Núñez, and H. Asorey. Performance of the lagoon water cherenkov detectors to cosmic ray flux. *arXiv preprint arXiv:2010.14591*, 2020.
13. L. Desorgher. The magnetocosmics code. Technical report, Technical report, <http://cosray.unibe.ch/~laurent/magnetocosmics>, 2004.
14. J. J. Masías-Meza and S. Dasso. Geomagnetic effects on cosmic ray propagation under different conditions for buenos aires and marambio, argentina. *Sun and Geosphere*, 9:41–47, 2014.
15. C. C. Finlay, S. Maus, C. D. Beggan, T. N. Bondar, A. Chambodut, T. A. Chernova, A. Chulliat, V. P. Golovkov, B. Hamilton, M. Hamoudi, R. Holme, G. Hulot, W. Kuang, B. Langlais, V. Lesur, F. J. Lowes, H. Lühr, S. MacMillan, M. Manda, S. McLean, C. Manoj, M. Menvielle, I. Michaelis, N. Olsen, J. Rauberg, M. Rother, T. J. Sabaka, A. Tangborn, L. Töffner-Clausen, E. Thébaud, A. W. P. Thomson, I. Wardinski, Z. Wei, and T. I. Zvereva. International Geomagnetic Reference Field: the eleventh generation. *Geophysical Journal International*, 183:1216–1230, December 2010.
16. N. A. Tsyganenko. A model of the near magnetosphere with a dawn-dusk asymmetry 1. mathematical structure. *Journal of Geophysical Research: Space Physics*, 107(A8):SMP 12–1–SMP 12–15, 2002.
17. D. Heck, J. Knapp, J.N. Capdevielle, G. Schatz, and T. Thouw. Corsika: A monte carlo code to simulate extensive air showers. Technical Report FZKA 6019, Forschungszentrum Karlsruhe GmbH, 1998.

18. S. Ostapchenko. Monte carlo treatment of hadronic interactions in enhanced pomeron scheme: Qgsjet-ii model. *Physical Review D*, 83(1):014018, 2011.
19. S. Agostinelli, J. Allison, K. Amako, J. Apostolakis, , et al. Geant4 - a simulation toolkit. *Nuclear Instruments and Methods in Physics Research Section A: Accelerators, Spectrometers, Detectors and Associated Equipment*, 506(3):250–303, jul 2003.
20. A. Filevich, P. Bauleo, H. Bianchi, J.R. Martino, and G. Torlasco. Spectral-directional reflectivity of tyvek immersed in water. *Nuclear Instruments and Methods in Physics Research Section A: Accelerators, Spectrometers, Detectors and Associated Equipment*, 423(1):108–118, 1999.
21. D. Allard, I. Allekotte, C. Alvarez, H. Asorey, H. Barros, X. Bertou, O. Burgoa, M. Gomez Berisso, O. Martínez, P. Miranda Loza, T. Murrieta, G. Pérez, H. Rivera, A. Rovero, O. Saavedra, H. Salazar, J.C. Tello, R. Ticona Peralda, A. Velarde, and L. Villaseñor. Use of water-cherenkov detectors to detect gamma ray bursts at the large aperture GRB observatory (lago). *Nuclear Instruments and Methods in Physics Research Section A: Accelerators, Spectrometers, Detectors and Associated Equipment*, 595(1):70 – 72, 2008. RICH 2007Proceedings of the Sixth International Workshop on Ring Imaging Cherenkov Detectors.
22. E. Huedo, R.S. Montero, and I.M. Llorente. The gridway framework for adaptive scheduling and execution on grids. *Scalable Computing: Practice and Experience*, 6(3), 2001.
23. M. Rodríguez-Pascual, R. Mayo-García, and I. M. Llorente. Montera: a framework for efficient execution of monte carlo codes on grid infrastructures. *Computing and Informatics*, 32(1):113–144, 2013.
24. A.J. Rubio-Montero, E. Huedo, F. Castejón, and R. Mayo-García. Gwpilot: Enabling multi-level scheduling in distributed infrastructures with gridway and pilot jobs. *Future Generation Computer Systems*, 45:25–52, 2015.
25. A.J. Rubio-Montero, E. Huedo, and R. Mayo-García. User-guided provisioning in federated clouds for distributed calculations. In *International Workshop on Adaptive Resource Management and Scheduling for Cloud Computing*, pages 60–77. Springer, 2015.
26. A.J. Rubio-Montero, R. Pagán-Muñoz, R. Mayo-García, A. Pardo-Díaz, I. Sidelnik, H. Asorey, and the LAGO Collaboration. The eoscsynergy cloud services implementation for the latin american giant observatory (lago). In *37th International Cosmic Ray Conference (ICRC2021)*, page PoS(ICRC2021)261, 2021.
27. M. Spurio. *Particles and Astrophysics*. Springer, 2014.
28. National Aeronautics and Space Administration. U.s. standard atmosphere 1976. Technical Report NASA-TM-X-74335, National Aeronautics and Space Administration (NASA), 1976.
29. P. Abreu, M. Aglietta, M. Ahlers, E.J. Ahn, I.F.M. Albuquerque, D. Allard, I. Allekotte, J. Allen, P. Allison, A. Almela, and The Pierre Auger Observatory. Description of atmospheric conditions at the pierre auger observatory using the global data assimilation system (gdas). *Astroparticle Physics*, 35(9):591–607, 2012.
30. J. Grisales-Casadiegos, C. Sarmiento-Cano, L.A. Nuñez, and the LAGO Collaboration. Gdas atmospheric models in astroparticle shower simulations. In *37th International Cosmic Ray Conference (ICRC2021)*, page PoS(ICRC21) 487, 2021.
31. A. Aab, P. Abreu, M. Aglietta, E.J. Ahn, I. Al Samarai, I.F.M. Albuquerque, I. Allekotte, J. Allen, P. Allison, A. Almela, and The Pierre Auger Collaboration. Depth of maximum of air-shower profiles at the pierre auger observatory. ii. composition implications. *Physical Review D*, 90(12):122006, 2014.



**Table 1.** Distribution of primaries to be simulated for a secondary flow of 120 s at the height of Bucaramanga obtained by ARTI.

Nuclei	Quantity	Nuclei	Quantity
H	562322	Al	44
He	56595	Na	38
C	1458	Ca	30
O	1410	F	25
Li	574	Cr	19
B	396	Ar	18
Mg	335	Ti	17
Si	322	Mn	13
N	295	K	11
Ne	259	V	10
Fe	195	P	9
Be	167	Cl	8
S	51	Sc	5

**Fig. 1.** The logical sequence is used to extract and build the 12-month average profiles for the city of Bucaramanga for 2018.

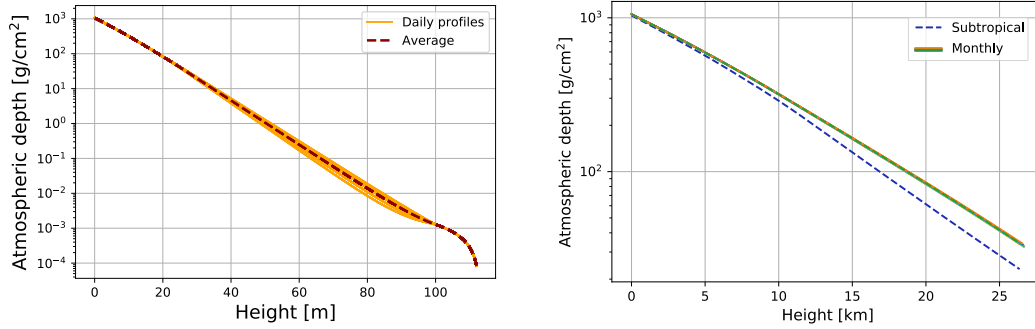


**Fig. 2.** Left panel shows as solid lines 62 density GDAS profiles for January at Bucaramanga ( $7.13^\circ$  N,  $73.00^\circ$  W) and the in-dash line, their average. The right side illustrates the first 30 km of the GDAS month density profiles for Bucaramanga and CORSIKA-tropical summer default profiles.

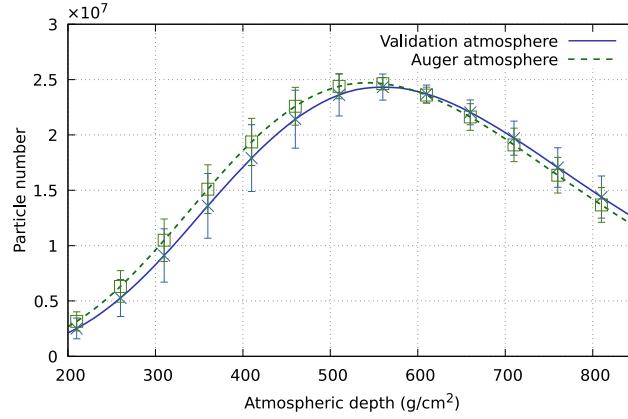


**Fig. 3.** Longitudinal distribution of secondary particles resulting from the interaction of an iron nucleus of  $1 \times 10^8$  GeV over the atmosphere of Malargüe for April. The Pierre Auger Observatory model in green and the atmosphere in the same conditions built by the methodology implemented for this work (Blue). As it can be seen, the differences in this parameter did not exceed 2% on both values of  $X_{max}$ .

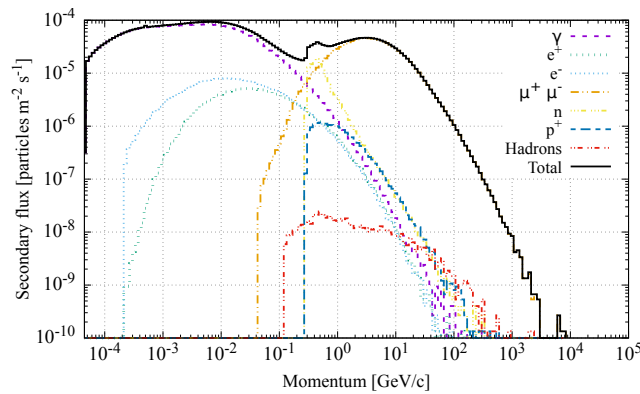


**Fig. 4.** Simulation of the energy spectrum of secondaries, at the level of Bucaramanga, using the atmospheric profile of April. The solid line represents the total secondary spectrum, and the dashed lines represent the contribution of photons, electrons, positrons, muons, neutrons, and protons separately.

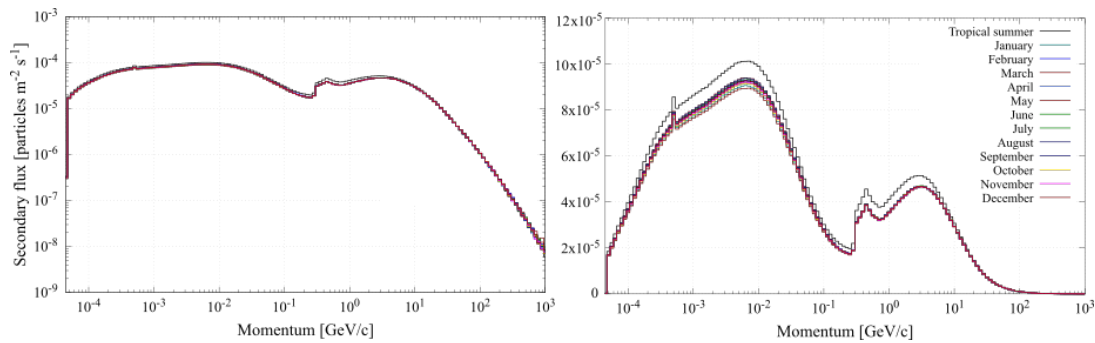


**Fig. 5.** Simulation of total secondary flux as a function of energy at Bucaramanga, using different means of interaction. The flux is in a logarithmic scale (left) and linear (right). In both cases, the black line represents the tropical summer profile, and the others correspond to the 12 monthly atmospheric profiles. The calculations show a overestimation of the tropical profile compared to the 12 GDAS atmospheres.

## A. Appendix

The following algorithm represents the three main parts that make up ARTI for flux simulations at CORSIKA, magnetic field correction via Magnetocosmic and detector simulation via Geant4 (See reference [12] for a more detailed description).

Simulation flux;

**Input** :  $E = [1, 10^6]$  GeV; energy range  
 injected primary nuclei,  $Z = [1, 26]$   
 $\theta = [0, 90]$ ; zenith angle range  
 $\phi = [-180, 180]$ ; azimuth angle range  
 Altitude in m a.s.l.  
 $B_x, B_z$ ; site's magnetic field  
 GDAS model; atmospheric model  
 time; 86400 sec in this case

**Output:**  $\Xi$ , particle flux at ground

**begin**

$\Phi(E_p, Z, A, \Omega)$ ; Integrate astroparticles spectra  
      $Z, \#part(E) \rightarrow$  built steering Corsika files  
     run block, via Corsika software  
     Analisis block; read and uncompress binary files

**end**

return  $\Xi$ ;

Magnetic field correction;

**Input** :  $\Xi$ , particle flux at ground  
            $R_m$ , magnetic rigidity  
           IGRF, magnetic model

**Output:**  $\Xi_{corr}$ , particle flux at ground corrected

**begin**

$R_C(\phi, \theta)$ , magnetic rigidity cutoff

**end**

return  $\Xi_{corr}$ ;

Magnetic field correction;

**Input** :  $\Xi_{corr}$ , particle flux at ground corrected  
            $D(r, h)$ , detector's dimensions  
           PMT, photo-multiplier's features

**Output:**  $E_D$ , energy deposited

**for particles do**

    interacting with water  
      $E_i^D$ , energy deposited by i-particle

**end**

return  $E_D$ ;

**Algorithm 1:** ARTI is divided in three parts. Flux simulations via Corsika, magnetic field correction via Magnetocsmic and detector simulation via Geant4